

A new approach to large-eddy simulations of wall-bounded turbulence using a fixed-width filter

By S. Ghosal,[†] R. Agrawal, A. Elnahhas AND P. Johnson[‡]

A new formulation of LES is proposed in which the filter width is fixed. The unfiltered or primitive field is defined in the entire domain that includes the solid and fluid phases. It obeys the Navier-Stokes equations for a Newtonian fluid but with a body force term that constrains the fluid velocity to match the velocity in the solid. The primitive field is then filtered using a fixed width filter to generate two LES fields (a) a volume LES (V-LES) defined at interior points in the fluid domain (b) a surface LES (S-LES) defined on points on the solid-fluid interface. Both V-LES and S-LES have unclosed terms that require subgrid models. The V-LES and S-LES fields are evolved concurrently and exchange information through boundary and source terms. The model is compared to previously published DNS and LES of turbulent channel flow.

1. Introduction

The basis of the LES approach is the decomposition of the turbulent field into resolved large-scale motion dependent on flow geometry and universal subgrid scales that can be described by simple models. As boundaries are approached, the distance to the boundary becomes the relevant length separating large and small scales. Thus, if subgrid scales are to be universal, LES must use spatially variable filter sizes and achieve DNS like resolution near walls. This would make LES computations of wall-bounded flows very expensive (Choi & Moin 2012). Another difficulty arises as a spatially variable filter introduces new terms into the standard LES equations (Ghosal & Moin 1995). A mathematically consistent formulation of LES that accounts for the effects of a variable filter width in a way that can be practically implemented has not yet been found.

The objective of this project is to redefine LES in a different way so as to overcome both of these limitations. We do this by relaxing the requirements that the subgrid scales be universal and that the LES approach DNS-like fidelity near boundaries. In the new approach, we reject the idea of a spatially variable filter and insist that we have a fixed filter size Δ and a corresponding filtering operation that is the same at all points in the domain. Our formalism differs from wall-modeled LES (Bose & Park 2018) approaches where one uses the LES velocity field at a grid point adjacent to the surface to infer a wall stress and then uses this wall stress as a boundary condition for the LES. Here, tangential and normal velocities for the V-LES field are given at the surface as Dirichlet-type conditions, as in DNS, but these components are nonzero at a solid stationary surface.

The remainder of this report is structured as follows. In Section 2, the new approach is formulated along the lines briefly outlined above. In Section 3, computational results

[†] Department of Mechanical Engineering, Northwestern University

[‡] Department of Mechanical and Aerospace Engineering, University of California, Irvine

are presented for a prototypical problem: turbulent flow in a planar channel. Finally, a summary and conclusions are provided in Section 4.

2. Formulation

We are concerned with domains that are partly occupied by a Newtonian viscous fluid and partly by rigid solids. We will pretend as if the whole volume (solid and fluid phases) is filled with a viscous fluid but with a space-time-dependent force density (force per unit mass) \mathbf{f} . The force \mathbf{f} is zero in the parts physically occupied by the fluid, but within the solid zone the force is such as to make the flow velocity go to zero rapidly as the solid-fluid boundary is crossed. We will assume a diffuse interface; that is, the force \mathbf{f} varies rapidly but continuously across the solid-fluid interface. A porous medium would be one physical example where such a force field exists. However, in our analysis, the force field exists only as an artifice that we use to arrive at our final equations. Once that is achieved, the fictitious body force does not enter our analysis again.

2.1. Volume LES formulation

We now apply a 3D fixed width filter of size Δ to the above equations to get the usual filtered LES equations in terms of the filtered velocity and pressure fields $\mathbf{V} = \bar{\mathbf{u}}$ and $P = \bar{p}$ and the subgrid stress $\boldsymbol{\tau}$. Here the filtered force $\bar{\mathbf{f}}$ that is small but nonzero near the boundary is dropped from the right-hand side. The boundary conditions on the V-LES are

$$\mathbf{V} \cdot \hat{\mathbf{n}} = V_n, \quad (2.1)$$

$$\mathbf{V} - (\mathbf{V} \cdot \hat{\mathbf{n}})\hat{\mathbf{n}} = \mathbf{u}, \quad (2.2)$$

on the bounding surface S with unit wall normal $\hat{\mathbf{n}}$. The 2D surface velocity \mathbf{u} along the surface and the vertical transpiration velocity V_n are discussed in the next section. From the perspective of V-LES, these quantities are supplied externally.

2.2. Surface LES formulation

The S-LES field is a 2D vector field $\mathbf{u}(\xi, \eta, t)$, that exists on the bounding surface S equipped with a (ξ, η) set of generalized surface coordinates. The evolution is described by a model

$$\partial_t \mathbf{u} = \mathbf{S}[\mathbf{u}]. \quad (2.3)$$

The operator \mathbf{S} would in general depend on certain V-LES features such as the shear stress at the wall. Developing suitable forms for \mathbf{S} is the task of S-LES modeling.

2.2.1. Equilibrium boundary layer

For the moment, we assume that the LES filter is a simple volume average over a cube of edge length Δ . This is adopted at present for simplicity but may be replaced by a different filtering kernel. We assume that the velocity below the surface rapidly goes to zero due to the assumed body force term \mathbf{f} . Thus, we must have at a point on the surface S

$$\langle \bar{u} \rangle = \frac{1}{\Delta} \int_0^{\Delta/2} \langle u \rangle dy. \quad (2.4)$$

Here y denotes the wall-normal direction, and $\langle \ \rangle$ denotes ensemble or Reynolds average. We now assume that the averaged streamwise velocity may be approximated by the law

of the wall. Thus, in the region $(0, \Delta)$,

$$\frac{\langle u \rangle}{u_\tau} = u_+ = f(y_+), \quad (2.5)$$

where $f(y_+)$ is a suitable analytical formula describing the boundary layer profile in terms of the wall-normal coordinate in wall units $y_+ = u_\tau y / \nu$. Here $u_\tau = \sqrt{\tau_w / \rho}$, where τ_w is the shear stress at the wall. We define

$$F(\Delta_+) = \frac{1}{\Delta_+} \int_0^{\Delta_+/2} f(y_+) dy_+. \quad (2.6)$$

Thus, we require our specified ‘slip’ velocity to satisfy

$$\frac{\langle \bar{u} \rangle}{u_\tau} = \frac{1}{\Delta} \int_0^{\Delta/2} \frac{\langle u \rangle}{u_\tau} dy = \frac{1}{\Delta_+} \int_0^{\Delta_+/2} f(y_+) dy_+ = F(\Delta_+). \quad (2.7)$$

A simple expression for $F(\Delta_+)$ can be constructed by considering the boundary layer to consist of a viscous sublayer, buffer layer, and log layer as in the Reichardt model (Lehmkuhl et al. 2018):

$$f(y_+) = \frac{1}{\kappa} \ln(1 + \kappa y_+) + A(1 - e^{-\alpha y_+} - \alpha y_+ e^{-\beta y_+}), \quad (2.8)$$

where $A = 7.8$, $\alpha = 1/11 \approx 0.0909$ and $\beta = 0.33$ are numerical constants. The integration in this case can be performed analytically and results in

$$\begin{aligned} F(\Delta_+) &= \frac{1}{2\kappa} \left[\left(1 + \frac{2}{\kappa \Delta_+} \right) \ln \left(1 + \frac{\kappa \Delta_+}{2} \right) - 1 \right] + \frac{A}{2} - \frac{A}{\alpha \Delta_+} \left(1 - e^{-\alpha \Delta_+/2} \right) \\ &\quad - \frac{\alpha A}{\beta^2 \Delta_+} \left(1 - e^{-\beta \Delta_+/2} \right) + \frac{\alpha A}{2\beta} e^{-\beta \Delta_+/2}. \end{aligned} \quad (2.9)$$

2.2.2. Non-equilibrium boundary layer

In the general case of a non-equilibrium boundary layer, we must determine an equation for the field \mathbf{u} by starting from the underlying Navier-Stokes equations with the body force term.

We start by writing the basic equations in a locally flat coordinate system on the surface S with x_3 orthogonal to the surface and x_1 and x_2 in any two mutually orthogonal directions that lie on the tangent plane. In what follows, we will use the Einstein summation convention but with indices running over 1, 2, 3, for Latin letters (i, j, k, \dots) but over 1, 2, for Greek letters (α, β, \dots). We will for the moment use overbars to indicate the filtered field, but these bars will be dropped when we write the final equations for the 2D S-LES field. Thus, the filtered Navier-Stokes equations with this convention appear as

$$\partial_t \bar{u}_\alpha + (\bar{u}_\beta \bar{u}_\alpha)_{,\beta} + (\bar{u}_3 \bar{u}_\alpha)_{,3} = -\bar{p}_{,\alpha} / \rho + \nu \bar{u}_{\alpha,\beta\beta} + \nu \bar{u}_{\alpha,33} + \bar{f}_\alpha, \quad (2.10)$$

$$\bar{u}_{\alpha,\alpha} + \bar{u}_{3,3} = 0, \quad (2.11)$$

where a comma signifies differentiation with respect to the indices that follow. We will now rewrite some of the terms in the above equations. To do this, we will evaluate the filter in the x_3 direction while using the tilde to indicate the remaining filtering with respect to the x_1 - x_2 plane.

First consider the last term in the continuity equation

$$\bar{u}_{3,3} = \frac{1}{\Delta} \int_{-\Delta/2}^{+\Delta/2} \tilde{u}_{3,3} dx_3 = \frac{1}{\Delta} \tilde{u}_3|_{x_3=\Delta/2}. \quad (2.12)$$

This term represents the volume flux out of the wall region and must equal V_n in Eq. (2.1). Therefore, using the continuity equation,

$$V_n = V_3 = -\Delta \bar{u}_{\alpha,\alpha}. \quad (2.13)$$

2.2.3. The driving stress term

The third term on the left-hand side of Eq. (2.10) may be written as

$$(\overline{u_3 u_\alpha})_{,3} = \frac{1}{\Delta} \int_{-\Delta/2}^{+\Delta/2} (\widetilde{u_3 u_\alpha})_{,3} dx_3 = \frac{1}{\Delta} \widetilde{u_3 u_\alpha}|_{x_3=\Delta/2}. \quad (2.14)$$

The third term on the right side of Eq. (2.10) may be written as

$$\nu \bar{u}_{\alpha,33} = \frac{\nu}{\Delta} \int_{-\Delta/2}^{+\Delta/2} \tilde{u}_{\alpha,33} dx_3 = \frac{\nu}{\Delta} \tilde{u}_{\alpha,3}|_{x_3=\Delta/2}. \quad (2.15)$$

The boundary terms can be combined into a single term on the right hand side

$$\left[\frac{\nu}{\Delta} \tilde{u}_{\alpha,3} - \frac{1}{\Delta} \widetilde{u_3 u_\alpha} \right]_{x_3=\Delta/2} = \frac{1}{\rho \Delta} [\mu \tilde{u}_{\alpha,3} - \rho \widetilde{u_3 u_\alpha}]_{x_3=\Delta/2}. \quad (2.16)$$

This may be related to the total stress in the V-LES field on S. Indeed, the $(3, \alpha)$ component of the total stress is

$$T_{3\alpha} = \tau_{3\alpha} + \tau_{3\alpha}^v - \rho \bar{u}_3 \bar{u}_\alpha, \quad (2.17)$$

where

$$\tau_{3\alpha} = \rho(\bar{u}_3 \bar{u}_\alpha - \overline{u_3 u_\alpha}) \quad (2.18)$$

is the subgrid stress,

$$\tau_{3\alpha}^v = \mu(\bar{u}_{3,\alpha} + \bar{u}_{\alpha,3}) \approx \mu \bar{u}_{\alpha,3} \quad (2.19)$$

is the viscous stress, and the last term is the resolved part of the convective stress. The term $\bar{u}_{3,\alpha}$ has been dropped from the viscous stress as it is small compared with the remaining term for points near the bounding surface S. If we disregard the difference between the 2D and 3D filtering, we now have

$$[\mu \tilde{u}_{\alpha,3} - \rho \widetilde{u_3 u_\alpha}]_{x_3=\Delta/2} \approx [\mu \bar{u}_{\alpha,3} - \rho \overline{u_3 u_\alpha}]_{x_3=\Delta/2} = [\tau_{3\alpha}^v + \tau_{3\alpha} - \rho \bar{u}_3 \bar{u}_\alpha]_S = T_{3\alpha}|_S. \quad (2.20)$$

On replacing the boundary terms by the total stress in Eq. (2.10), we get

$$\partial_t \bar{u}_\alpha + (\overline{u_\alpha u_\beta})_{,\beta} = -\bar{p}_{,\alpha}/\rho + \nu \bar{u}_{\alpha,\beta\beta} + \frac{T_{3\alpha}|_S}{\rho \Delta} + \bar{f}_\alpha. \quad (2.21)$$

2.2.4. The filtered body force term

The body force term that ensures that the fluid velocity goes to zero rapidly on crossing S has not been discussed in detail thus far. We now introduce a simple model for this body force,

$$f_\alpha = \begin{cases} -\kappa u_\alpha, & \text{if } x_3 \leq 0 \\ 0, & \text{if } x_3 > 0 \end{cases} \quad (2.22)$$

where $\kappa > 0$ is a parameter that is sufficiently large that the velocity decays very rapidly below the surface S. Vertical equilibrium implies that the pressure gradient $p_{,\alpha}$ is independent of x_3 . Neglecting inertial terms and gradients in x_1 and x_2 , we have, for $x_3 < 0$,

$$\nu u_{\alpha,33} - \kappa u_{\alpha} = p_{,\alpha}/\rho, \quad (2.23)$$

which has the solution

$$u_{\alpha} = u_{\alpha}|_{x_3=0} \exp(\sqrt{\kappa/\nu} x_3) - p_{,\alpha}/(\kappa\rho). \quad (2.24)$$

The filtered force may now be evaluated

$$\bar{f}_{\alpha} = -\frac{1}{\Delta} \int_{-\Delta/2}^0 \kappa u_{\alpha} dx_3 = -\frac{1}{\Delta} \int_{-\Delta/2}^0 \kappa u_{\alpha}|_{x_3=0} \exp[\sqrt{\kappa/\nu} x_3] dx_3 + \frac{1}{2} \frac{p_{,\alpha}}{\rho} \quad (2.25)$$

$$= -\frac{\sqrt{\kappa\nu}}{\Delta} u_{\alpha}|_{x_3=0} \left[1 - e^{-\frac{\Delta}{2}\sqrt{\kappa/\nu}} \right] + \frac{1}{2} \frac{p_{,\alpha}}{\rho} \sim -\frac{\sqrt{\kappa\nu}}{\Delta} u_{\alpha}|_{x_3=0} + \frac{1}{2} \frac{p_{,\alpha}}{\rho}, \quad (2.26)$$

where the last term indicates the asymptotic limit of large κ . We wish to relate the quantity $u_{\alpha}|_{x_3=0}$ to the filtered velocity at the wall $\bar{u}_{\alpha}|_{x_3=0}$. If κ is large, there is a very rapid decay of the velocity when $x_3 < 0$ and, if the velocity changes little over the region $(0, \Delta/2)$, then we would have $\bar{u}_{\alpha}|_{x_3=0} \approx u(x_3 = 0)/2$. In general, we could write

$$\bar{u}_{\alpha} = \frac{1}{2} c u_{\alpha}(x_3 = 0), \quad (2.27)$$

where c is, for the present, an undetermined parameter. Thus, finally we have the required filtered force on the surface S

$$\bar{f}_{\alpha} = -\frac{2\sqrt{\kappa\nu}}{c\Delta} \bar{u} + \frac{1}{2} \frac{\bar{p}_{,\alpha}}{\rho}, \quad (2.28)$$

where we have replaced the surface pressure with the filtered pressure.

2.2.5. The surface subgrid stress

Returning to Eq. (2.21), we note that the term $\overline{u_{\alpha}u_{\beta}}$ on the left-hand side is unclosed. Following the usual process of subgrid modeling, we write

$$\overline{u_{\alpha}u_{\beta}} = \bar{u}_{\alpha}\bar{u}_{\beta} - \frac{\sigma_{\alpha\beta}}{\rho}, \quad (2.29)$$

where

$$\sigma_{\alpha\beta} = \rho(\bar{u}_{\alpha}\bar{u}_{\beta} - \overline{u_{\alpha}u_{\beta}}) \quad (2.30)$$

is a term that represents the subgrid transfer of horizontal momentum along the surface S. Note that

$$\frac{\sigma_{\gamma\gamma}}{2} = \frac{\rho}{2}(\bar{u}_{\alpha}\bar{u}_{\alpha} - \overline{u_{\alpha}u_{\alpha}}) = -k, \quad (2.31)$$

where k is the subgrid kinetic energy in the 2D surface flow. One could separate out the trace-free part of the S-LES stress by defining the deviatoric part

$$\sigma_{\alpha\beta}^* = \sigma_{\alpha\beta} - \frac{\delta_{\alpha\beta}}{2} \sigma_{\gamma\gamma} = \sigma_{\alpha\beta} + k\delta_{\alpha\beta}. \quad (2.32)$$

Since the 2D surface flow is not solenoidal, we need subgrid models for both k and $\sigma_{\alpha\beta}^*$. The development of such S-LES subgrid models is an enterprise on its own. Only very simple models will be considered in this report.

2.2.6. Pressure equilibrium

Equation (2.21) still contains the pressure term, which we are now going to relate to the pressure in the V-LES field. To do this, we write the vertical component of the momentum equation for a point lying on the surface

$$\partial_t \bar{u}_3 + (\overline{u_\alpha u_3})_{,\alpha} + (\overline{u_3 u_3})_{,3} = -\bar{p}_{,3}/\rho + \nu \bar{u}_{3,\alpha\alpha} + \nu \bar{u}_{3,33}. \quad (2.33)$$

The filtered force component \bar{f}_3 has already been dropped from the right-hand side since there is no velocity in the x_3 direction below the surface and no pressure gradient components. We now transform the terms involving total derivatives with respect to x_3 in the usual way by regarding the 3D filter as a product of 1D filters in each of the three directions and evaluating the filter in the x_3 direction explicitly. Thus, we have

$$\begin{aligned} \partial_t \bar{u}_3 + (\overline{u_\alpha u_3})_{,\alpha} + \frac{1}{\Delta} \widetilde{u_3 u_3}|_{x_3=\Delta/2} &= -\frac{1}{\rho\Delta} \left[\tilde{p}|_{x_3=\Delta/2} - \tilde{p}|_{x_3=0} \right] \\ &+ \nu \bar{u}_{3,\alpha\alpha} + \frac{\nu}{\Delta} \tilde{u}_{3,3}|_{x_3=\Delta/2}. \end{aligned} \quad (2.34)$$

Here we have made use of the fact that the pressure is constant in the zone $(-\Delta/2, 0)$. We will now examine the size of each of these terms following the usual boundary-layer-type assumption that variables change slowly in the horizontal directions over a length scale L but rapidly in the vertical direction over the length scale Δ . Thus, $\partial_\alpha \sim 1/L$ but $\partial_3 \sim 1/\Delta$. We will assume that $u_\alpha \sim u_\tau$ but $u_3 \sim (\Delta/L)u_\tau$ in view of the continuity equation. The timescale for the variation of surface fields is L/u_τ ; therefore, $\partial_t \sim u_\tau/L$. Thus, we arrive at the following estimates for the various terms in the above equation

$$\partial_t \bar{u}_3 \sim (\overline{u_\alpha u_3})_{,\alpha} \sim \widetilde{u_3 u_3}|_{x_3=\Delta/2} \sim (\Delta/L)(u_\tau^2/L),$$

$$\nu \bar{u}_{3,\alpha\alpha} \sim (1/\Delta_+)(\Delta/L)^2(u_\tau^2/L), \quad (\nu/\Delta)\tilde{u}_{3,3}|_{x_3=\Delta/2} \sim (1/\Delta_+)(u_\tau^2/L).$$

All of these terms are order (Δ/L) or smaller and may be dropped. The last term may be dropped because our filter width is presumed to be much larger than the laminar boundary layer thickness, so that $\Delta_+ \gg 1$. However, in what follows we will retain the small boundary term $(1/\Delta)\widetilde{u_3 u_3}|_{x_3=\Delta/2}$. The reasons for doing so are: (a) Retaining the term does not lead to any additional complexity and may easily be handled, and (b) it makes our equations closely follow the classical Reynolds-averaged Navier-Stokes (RANS) analysis for planar channels. Setting $\tilde{p}|_{x_3=\Delta/2} = P$, $\tilde{p}|_{x_3=0} = \bar{p}$, we have

$$\bar{p} = P + \rho \widetilde{u_3 u_3}|_{x_3=\Delta/2} = P + \rho V_3 V_3 - \tau_{33}, \quad (2.35)$$

which may be rewritten in a form that only contains the modified pressure $P - (\tau_{kk}/3) = P + (2/3)K$, where K is the subgrid kinetic energy in the V-LES field,

$$\bar{p} = P + \frac{2}{3}K + \rho V_3 V_3 - \tau_{33}^*. \quad (2.36)$$

Note that the last two terms in the above equation for pressure are of the same order as other neglected terms in the equation and may safely be dropped if desired. These terms are retained in the usual RANS analysis of channel flow because that analysis is exact and does not involve dropping any small terms.

2.2.7. The surface flow equations

Now, using Eqs. (2.29)-(2.28) in Eq. (2.21), we have

$$\partial_t \bar{u}_\alpha + (\bar{u}_\beta \bar{u}_\alpha)_{,\beta} = -\frac{1}{\rho} \left(\frac{\bar{p}}{2} + k \right)_{,\alpha} + \frac{\sigma_{\alpha\beta,\beta}^*}{\rho} + \nu \bar{u}_{\alpha,\beta\beta} + \frac{T_{3\alpha}|_S}{\rho\Delta} - \frac{2\sqrt{\kappa\nu}}{c\Delta} \bar{u}_\alpha. \quad (2.37)$$

Our equation still has an undetermined parameter, $\sqrt{\kappa}/c$. We will now determine this parameter by demanding that Eq. (2.37) provide the correct equilibrium boundary layer result in Eq. (2.7) in the situation where the turbulence near the wall is statistically steady and its statistical properties do not vary in directions parallel to the wall.

We first take an ensemble average of both sides of Eq. (2.37),

$$\partial_t \langle \bar{u}_\alpha \rangle + \langle \bar{u}_\beta \bar{u}_\alpha \rangle_{,\beta} = -\frac{\langle \bar{p}/2 + k \rangle_{,\alpha}}{\rho} + \frac{\langle \sigma_{\alpha\beta}^* \rangle_{,\beta}}{\rho} + \nu \langle \bar{u} \rangle_{\alpha,\beta\beta} + \frac{\langle T_{3\alpha} \rangle|_S}{\rho\Delta} - \frac{2\sqrt{\kappa\nu}}{c\Delta} \langle \bar{u}_\alpha \rangle. \quad (2.38)$$

Under the assumption of statistically steady turbulence that is invariant in directions parallel to the wall, all of the terms in the above equation are clearly zero except for the last two terms on the right. Equation (2.38) now reduces to

$$\frac{\langle T_{3\alpha} \rangle|_S}{\rho\Delta} - \frac{2\sqrt{\kappa\nu}}{c\Delta} \langle \bar{u}_\alpha \rangle = 0. \quad (2.39)$$

Here we have neglected the mean pressure gradient term $\langle P \rangle_{,\alpha}$. This is because force balance requires the mean pressure gradient $-\langle P \rangle_{,\alpha} \sim \tau_w/R$, where R is a characteristic geometrical dimension of the flow. For example, for a channel flow, $R = H$, the channel half-width. For flow through a conduit of cross-sectional area A and length L containing any number of objects, force balance requires

$$-\langle P \rangle_{,\alpha} AL \sim \tau_w S, \quad (2.40)$$

where S is the wetted surface area and τ_w is a characteristic shear stress. Thus, $-\langle P \rangle_{,\alpha} \sim \tau_w/R$, where $R = AL/S$ is a characteristic geometric dimension of the simulation. Thus, the ratio of the pressure gradient term to the last two terms in Eq. (2.38) $\sim \Delta/R$. This ratio must be small as the filter size needs to be much smaller than the characteristic geometric scale for the simulation to be meaningful. Therefore neglect of the mean pressure gradient term is justified.

Substituting in Eq. (2.39) results in a solution for the ensemble-averaged S-LES field that is proportional to the average total wall shear stress in the V-LES field

$$\langle \bar{u}_\alpha \rangle = \frac{1}{2} \frac{c}{\sqrt{\kappa\nu}} \frac{\langle T_{3\alpha} \rangle|_S}{\rho}. \quad (2.41)$$

It is convenient to take the dot product with the mean velocity

$$\langle \bar{u}_\alpha \rangle \langle \bar{u}_\alpha \rangle = \frac{1}{2} \frac{c}{\sqrt{\kappa\nu}} \frac{\langle T_{3\alpha} \rangle|_S \langle \bar{u}_\alpha \rangle}{\rho}, \quad (2.42)$$

so that

$$\frac{\sqrt{\kappa}}{c} = \frac{1}{2} \frac{1}{\rho\sqrt{\nu}} \frac{\langle T_{3\alpha} \rangle|_S \langle \bar{u}_\alpha \rangle}{\langle \bar{u}_\alpha \rangle \langle \bar{u}_\alpha \rangle}. \quad (2.43)$$

Since this is a scalar equation, the right hand side can be evaluated in an arbitrarily rotated coordinate system on the surface S . Let us assume that we have oriented the coordinate system so that the mean flow is in the x_1 direction. Then, if we require the

above solution to be consistent with Eq. (2.7), we obtain

$$\frac{\sqrt{\kappa}}{c} = \frac{1}{2\sqrt{\nu}} \frac{u_\tau}{F(y_+)}. \quad (2.44)$$

The parameter u_τ can be written, once again appealing to rotational invariance of the dot product, as

$$u_\tau^2 = \frac{\langle T_{3\alpha} \rangle|_S \langle T_{3\alpha} \rangle|_S}{\rho} \quad (2.45)$$

or

$$u_\tau = \sqrt{\langle T_{3\alpha} \rangle|_S \langle T_{3\alpha} \rangle|_S / \rho}. \quad (2.46)$$

On substituting the now determined parameter $\sqrt{\kappa}/c$ in Eq. (2.37), we get

$$\partial_t \bar{u}_\alpha + (\bar{u}_\beta \bar{u}_\alpha)_{,\beta} = -\frac{(\bar{p}/2 + k)_{,\alpha}}{\rho} + \frac{\sigma_{\alpha\beta,\beta}^*}{\rho} + \nu \bar{u}_{\alpha,\beta\beta} + \frac{1}{\rho\Delta} \left[T_{3\alpha}|_S - \frac{\rho u_\tau \bar{u}_\alpha}{F(\Delta_+)} \right], \quad (2.47)$$

with u_τ given by Eq. (2.46). Note that the term $T_{3\alpha}|_S$ is a fluctuating stress that drives the S-LES field. It is different from the mean total stress $\langle T_{3\alpha} \rangle|_S$. Since the ensemble average is not available in an LES, the $\langle \ \rangle$ in the total stress will need to be replaced by a local average on a disc several times larger than the filter width.

2.3. Generalized coordinates

Our equations so far have been written in a locally flat coordinate system. It is helpful to rewrite them in a form so that any (not necessarily orthogonal) 2D body-fitted coordinate system can be used. We achieve this by replacing partial derivatives by covariant derivatives. For consistency, we also rewrite the vector source term so that it only has components along the surface. Thus, the final S-LES equations, written in standard vector notation, are

$$\partial_t \mathbf{u} + \nabla_S \cdot (\mathbf{u}\mathbf{u}) = -\frac{1}{\rho} \nabla_S \left(\frac{p}{2} + k \right) + \nu \nabla_S^2 \mathbf{u} + \frac{1}{\rho} \nabla_S \cdot \boldsymbol{\sigma}^* + \frac{\mathbf{S}}{\rho\Delta}, \quad (2.48)$$

where

$$p = P + \frac{2}{3}K + \rho(\hat{\mathbf{n}} \cdot \mathbf{V})^2 - \hat{\mathbf{n}} \cdot \boldsymbol{\tau}^* \cdot \hat{\mathbf{n}} \quad (2.49)$$

and

$$\mathbf{S} = \hat{\mathbf{n}} \cdot \mathbf{T} - \hat{\mathbf{n}}(\hat{\mathbf{n}} \cdot \mathbf{T} \cdot \hat{\mathbf{n}}) - \rho \mathbf{u} u_\tau / F(\Delta_+). \quad (2.50)$$

We have omitted the designation $|_S$ because all V-LES quantities appearing in S-LES equations are presumed evaluated on the surface S.

3. Validation

The formulation described above has some essential self consistency properties: (a) In the limit $\Delta \rightarrow 0$, the model reduces exactly to the equations for DNS, (b) the filtered parabolic profile is recovered for laminar flow in a planar channel, and (c) for any laminar flow past a bounding surface, the model reduces to the filtered laminar boundary layer profile corresponding to the local value of the shear stress. The S-LES solution for the slip velocity in this case is stable and collapses onto the correct value on a fast timescale. We omit the detailed proofs of these facts in this report for brevity.

To validate the model, we considered the case of LES of fully developed turbulent

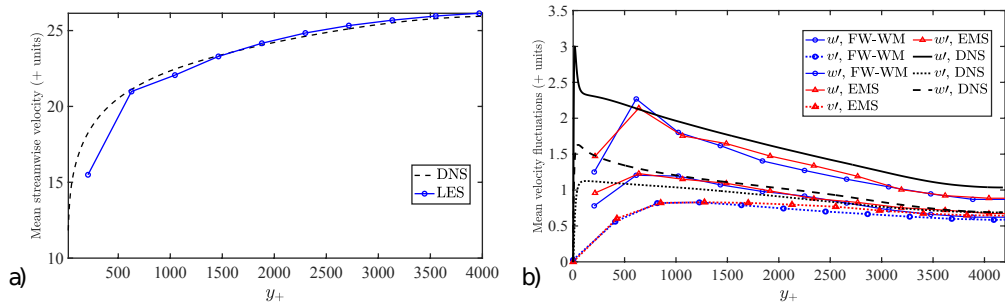


FIGURE 1. (a) Mean streamwise velocity and (b) turbulence intensity profiles in wall units. The current fixed filter width model (FW-WM) is compared with fully resolved simulations (DNS) and the exact mean stress (EMS) model. The Reynolds number $Re_\tau = 4200$.

channel flow. For this prototypical problem, we compared results with both DNS (Lozano-Durán & Jiménez 2014) and LES with the EMS (exact mean stress) model of Lozano-Durán & Bae (2019).

The computations were performed using a numerical solver that employs a second-order finite-difference approach with RK3 time-stepping. This solver has been used and extensively verified in many previous studies (Lozano-Durán & Bae 2019; Agrawal et al. 2022; Bae et al. 2018, 2019; Bae & Lozano-Durán 2021). A $64 \times 21 \times 32$ coarse staggered grid was used to simulate fully developed turbulence at $Re_\tau = 4200$. The filter as well as the grid size was 0.1 times the channel half-width. The channel length was twice the span and π times the channel height. The AMD (anisotropic minimum dissipation) model of Rozema et al. (2015) was adopted as the V-LES subgrid model.

As discussed earlier, the S-LES subgrid model needs to capture the boundary layer physics (Jodai & Elsinga 2016) that in the present approach operates below the resolved scales. We do not yet have such a model. For the purpose of this preliminary investigation, we adapted the V-LES model for the purpose of S-LES by utilizing a Neumann closure for the subgrid-stresses: The surface subgrid stresses were derived from a Neumann interpolation of the eddy viscosity from the wall-neighboring interior cell. This simplistic approach proved to be unstable in practice due to the appearance of sharp gradients in the S-LES fields. We found that the simulations could be run stably if the volume extrapolated eddy viscosity was amplified by a factor of 30 in an ad hoc manner. Once stabilized in this way, the simulations produced good agreement with DNS as well as with published LES data with the EMS model as shown in Figure 1 for the mean flow and turbulent intensity profiles.

4. Conclusions

A new approach to LES of wall-bounded turbulent flows using a fixed-width filter is presented. The primitive field is described by the Navier-Stokes equations in all space with a body force term that constrains the fluid velocity to match the known velocity in the solid. The final result is a set of coupled 3D LES equations defined in the volume (V-LES) and 2D LES equations defined on bounding surfaces (S-LES). The S-LES equations provide slip and transpiration boundary conditions to the V-LES, which in turn provide boundary values that appear as source terms in the S-LES equations. The proposed

formulation eliminates the requirement of resolving fine-scale eddies near boundaries and is free of complications associated with variable filter widths.

The approach was tested in a fully developed channel flow using very simple subgrid models. The tests provided partial validation of the approach. Good predictions of mean velocity and turbulence intensity profiles could be obtained, but only if the S-LES computation was stabilized in an ad hoc manner using artificially enhanced eddy viscosities. This finding was not entirely surprising, as one does not expect the structure of the two-dimensional surface subgrid stresses to necessarily resemble the corresponding V-LES subgrid stresses.

The work presented here is preliminary. The 2D pseudo-compressible S-LES equations appear to be susceptible to the formation of unphysical sharp gradients, likely due to the absence of a proper S-LES subgrid model. Therefore, future work needs to focus on the development of such models. Appropriate models must take account of the anisotropy in turbulence stresses and kinetic energy components that are characteristic of the physics of the turbulent boundary layer.

Acknowledgments

The authors acknowledge use of computational resources from the Yellowstone cluster awarded by the National Science Foundation to CTR.

REFERENCES

- AGRAWAL, R. ET AL. 2022 Non-Boussinesq subgrid-scale model with dynamic tensorial coefficients *Phys. Rev. Fluids* **7**(7), 074602.
- BAE, H. J., LOZANO-DURÁN, A., BOSE, S. T. & MOIN, P. 2018 Turbulence intensities in large-eddy simulation of wall-bounded flows *Phys. Rev. Fluids* **3**(1), 014610.
- BAE, H. J., LOZANO-DURAN, A., BOSE, S. T. & MOIN, P. 2019 Dynamic slip wall model for large-eddy simulation. *J. Fluid Mech.* **859**, 400–432.
- BAE, H. J. & LOZANO-DURÁN, A. 2021 Effect of Wall Boundary Conditions on a Wall-Modeled Large-Eddy Simulation in a Finite-Difference Framework. *Fluids* **6**(3), 112.
- BOSE, S. T. & PARK, G. I. 2018 Wall-Modeled Large-Eddy Simulation for Complex Turbulent Flows. *Ann. Rev. Fluid Mech.* **50**, 535–61.
- CHOI, H. & MOIN, P. 2012 Grid-point requirements for large eddy simulation: Chapman’s estimates revisited. *Phys. Fluids*. **24**, 011702.
- GHOSAL, S. & MOIN, P. 1995 The basic equations for the large eddy simulation of turbulent flows in complex geometry. *J. Comput. Phys.* **118**, 24–37.
- JODAI, Y. & ELSINGA, G. E. 2016 Experimental observation of hairpin auto-generation events in a turbulent boundarylayer. *J. Fluid Mech.* **795**, 611–633.
- LEHMKUHL, O., PARK, G. I., BOSE, S. T. & MOIN, P. 2018 Large-eddy simulation of practical aeronautical flows at stall conditions. *Proceedings of the Summer Program*, Center for Turbulence Research, Stanford University, pp. 87–96.
- LOZANO-DURÁN, A. & BAE, H. J. 2019 Error scaling of large-eddy simulation in the outer region of wall-bounded turbulence. *J. Comp. Phys.* **392**, 532–555.
- LOZANO-DURÁN, A. & JIMÉNEZ, J. 2014 Effect of the computational domain on direct simulations of turbulent channels up to $Re_\tau = 4200$ *Phys. Fluids*. **26**, 011702.
- ROZEMA, W. *et al.* 2015 Minimum-dissipation models for large-eddy simulation. *Phys. Fluids* **27**, 085107.